Chinese Chemical Letters 36 (2025) 110333

Contents lists available at ScienceDirect

Chinese Chemical Letters

journal homepage: www.elsevier.com/locate/cclet

Nanozyme-triggered polymerization amplification strategy for constructing highly sensitive surface plasmon resonance immunosensing

Feng Shi[a,1], Guiling Li[c,1], Haibing Zhu[a,1], Ling Li[a], Ming Chen[a], Juan Li[a], Huifang Shen[a], Hao Zeng[b,*], Lingfeng Min[c,*], Zhanjun Yang[a,*]

[a] School of Chemistry and Chemical Engineering, Yangzhou University, Yangzhou 225002, China
[b] National Engineering Research Center of Immunological, Department of Microbiology and Biochemical Pharmacy, College of Pharmacy and Laboratory Medicine, Third Military Medical University, Chongqing 400037, China
[c] Department of Respiratory and Critical Care Medicine, Northern Jiangsu People's Hospital, Clinical Medical College, Yangzhou University, Yangzhou 225001, China

ARTICLE INFO

Article history:
Received 19 May 2024
Revised 1 July 2024
Accepted 9 August 2024
Available online 14 August 2024

Keywords:
Au@Pd core-shell nanooctahedra nanozyme
Polymerization amplification
POD-like activity
SPR immunosensor

ABSTRACT

Although diverse signal-amplified methods have been committed to improve the sensitivity of surface plasmon resonance (SPR) biosensing, introducing convenient and robust signal amplification strategy into SPR biosensing remains challenging. Here, a novel nanozyme-triggered polymerization amplification strategy was proposed for constructing highly sensitive surface plasmon resonance (SPR) immunosensor. In detail, Au@Pd core-shell nanooctahedra nanozyme with superior peroxidase (POD)-like activity was synthesized and utilized as a label probe. Simultaneously, Au@Pd core-shell nanooctahedra nanozyme can catalyze the decomposition of H_2O_2 to form hydroxyl radicals (·OH) that triggers the polymerization of aniline to form polyaniline attaching on the surface of sensor chip, significantly amplifying SPR responses. The sensitivity of SPR immunosensor was enhanced by nanozyme-triggered polymerization amplification strategy. Using human immunoglobulin G (HIgG) as a model, the constructed SPR immunosensor obtains a wide linear range of 0.005–1.0 μg/mL with low detection limit of 0.106 ng/mL. This research provides new sights on establishing sensitive SPR immunosensor and may evokes more inspiration for developing signal amplification methods based on nanozyme in biosensing.

Nanozymes, nanomaterials with intrinsic enzyme-like activity, have emerged to be a rapid-flourishing and diverse areas owing to their high stability, low cost, controllable activity and durability, which recuperates the limitations of natural enzymes utilizing in the application from biosensor to therapeutics [1-4]. Numerous nanomaterials with enzyme-like characteristics were investigated, including metal oxides [5-8], metal sulfides [9,10], metal-organic-frameworks [11-14], carbons [15-17] and noble metal [18-21] *etc*. Nowadays, nanozymes have been mainly utilized in colorimetric analysis [22,23], electrochemical sensing [24], chemiluminescence immunoassay [25,26] as well as photoelectrochemical immunoassay [27,28]. It is desirable to exploit new type of nanozymes and expand them to other biosensing fields. However, it is regrettable that nanozymes with intrinsic enzyme-like activities and optical properties have rarely been exploited to construct surface plasmon resonance biosensors.

Surface plasmon resonance (SPR), regarded as the promising methods for real-time detection of analytes [29], has received great interest attributed to its sensitivity, suitability as well as proper regeneration of sensor surface, which is widely utilized in disease diagnosis *via* establishing immunoassay analysis [30-32]. Although, a variety of efforts have been contributed to develop SPR immunosensor for quantifying biomolecules including biomarkers for disease [33,34], the inadequate sensitivity of the SPR immunosensor for extremely low concentration of biomolecules remains a challenge [35,36]. In the previous researches, various signal amplification strategies have been developed to increase SPR detection sensitivity including enzymatic amplification [37,38], atom transfer radical polymerization amplification [39,40] as well as introducing nanomaterials-labelled signal probe [41]. Intriguingly, polymerization signal amplification methods have become very pop-

* Corresponding authors.
E-mail addresses: zeng1109@163.com (H. Zeng), minlingfeng@126.com (L. Min), zjyang@yzu.edu.cn (Z. Yang).
[1] These authors contributed equally to this work.

https://doi.org/10.1016/j.cclet.2024.110333
1001-8417/

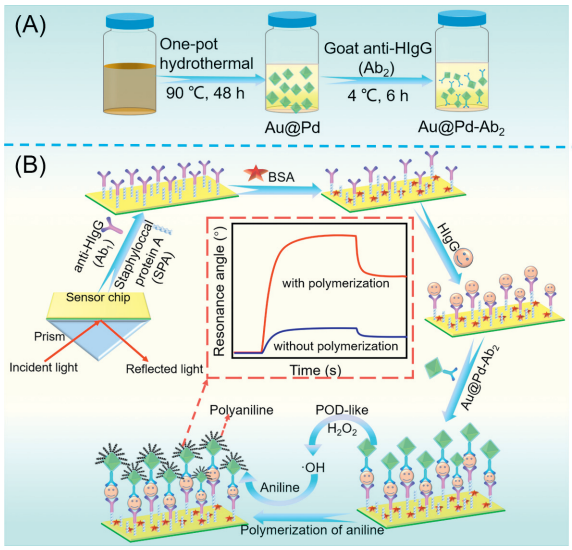

Scheme 1. (A) Preparation of Au@Pd core-shell nanooctahedra nanozyme and probe. (B) Schematic illustration of the sandwich immunoassay procedure of the SPR immunosensor.

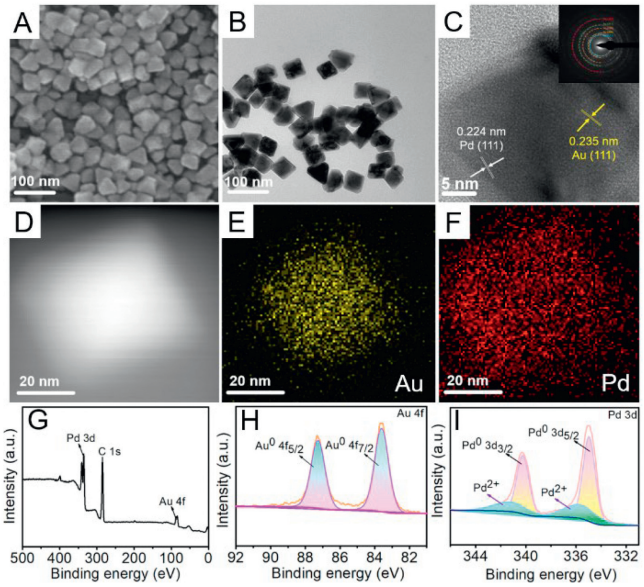

Fig. 1. (A) SEM image and (B) TEM image of Au@Pd core-shell nanooctahedra nanozyme. (C) High-resolution TEM image of Au@Pd core-shell nanooctahedra nanozyme. (D-F) HAADF-STEM and corresponding element mapping images. (G-I) Full XPS spectroscopy and high-resolution XPS spectra of Au@Pd core-shell nanooctahedra nanozyme.

ular due to the great signal amplification for improving sensitivity of SPR biosensors [42]. Nonetheless, the reported polymerization reaction mainly relies on excitation of natural enzymes, which has the shortcomings such as easy denaturation, instability in extreme environment, high cost in preparation and purification [43]. Moreover, the excitation polymerization process is relatively complex. These factors restrict the further development of the polymerization-induced signal amplification in SPR biosensor. Therefore, it is of great significance to incorporate nanozymes with polymerization strategy to fabricate efficient, highly sensitive and convenient signal amplification for SPR biosensing.

HIgG is considered as an important serum disease marker for diagnosis of several immune and chronic diseases. In this work, using HIgG as analyte model, a nanozyme-triggered polymerization amplification strategy was developed for constructing sensitive SPR immunosensing based on Au@Pd core-shell nanooctahedra nanozyme (Scheme 1). Secondary antibodies were loaded on Au@Pd core-shell nanooctahedra nanozyme to prepare SPR label probe (Au@Pd-Ab_2). The Au@Pd core-shell nanozyme shows superior peroxidase (POD)-like activity, and can catalyze the decomposition of H_2O_2 to form hydroxyl radicals (·OH), inducing the polymerization of aniline on the SPR chip to produce a remarkable amplification and promoting the SPR detection sensitivity. The proposed strategy compensates the shortcoming of current polymerization signal amplification methods and increases the sensitivity of SPR biosensing for extremely low concentration of biomolecules. Taken together, this work proposed an effective nanozyme-triggered polymerization amplification strategy for developing sensitive and convenient SPR immunosensing, which holds potential promise and enlarges the scope of nanozymes in biosensing.

The morphology and elemental composition of Au@Pd core-shell nanooctahedra nanozyme were investigated in Fig. 1. As can be seen from Figs. 1A and B, scanning electron micrographs (SEM) and transmission electron micrographs (TEM) images exhibit that Au@Pd core-shell nanooctahedra nanozyme with octahedral core-shell structure possesses uniform size of 60 nm. As shown in Fig. 1C, the high-resolution TEM image of Au@Pd core-shell nanooctahedra nanozyme exhibits two distinct fringes with spacings of 0.235 nm and 0.224 nm, corresponding to the (111) plane of Au and (111) facet of Pd, respectively, which preliminarily indicates that Pd mainly distributes outside while Au scatters inside. Figs. 1D-F demonstrate the high angle annular dark field scanning transmission electron microscope (HAADF-STEM) and corresponding element mapping images, declaring that the Au@Pd core-shell nanooctahedra nanozyme contains Pd (Fig. 1E) as outer shell and Au (Fig. 1F) element as inner core, which suggests the successful synthesis of Au@Pd core-shell nanooctahedra nanozyme. Energy dispersive X-Ray spectroscopy (EDX) and X-ray diffractometer (XRD) were utilized to characterize the successful preparation of Au@Pd nanozyme (Fig. S1 in Supporting information). X-ray photoelectron spectra (XPS) measurement was conducted to investigate the valence states of Au@Pd nanozyme. Fig. 1G exhibited a full XPS spectra of Au@Pd nanozyme, indicating the coexistence of Au and Pd. The high-resolution Au 4f spectra was deconvoluted into two peaks corresponding to Au^0 $4f_{7/2}$ and Au^0 $4f_{5/2}$with binding energies at 83.61 eV and 87.27 eV, respectively (Fig. 1H). The high-resolution Pd 3d spectra showed four peaks in Fig. 1I, including Pd^0 $3d_{5/2}$ (334.97 eV), Pd^0 $3d_{3/2}$ (340.28 eV), Pd^{2+} $3d_{5/2}$ (335.98 eV) and Pd^{2+} $3d_{3/2}$ (341.24 eV), suggesting that the Pd species in Au@Pd nanozyme are mostly in the valence state of Pd^0. The existence of few amounts of Pd^{2+} can be attributed to the absorption of surface oxygen on the Pd surface of Au@Pd nanozyme, further verifying the metallic state of the Pd shell and Au core [44].

3,3′,5,5′-Tetramethylbenzidine (TMB), regarded as typical chromogenic substrate, has been utilized to investigate the POD-like activity of Au@Pd core-shell nanooctahedra nanozyme. It can be seen obviously from Fig. 2A that a strong absorption peak occurs at 652 nm belonging to the mixed solution of the TMB+H_2O_2+Au@Pd core-shell nanooctahedra nanozyme (curve c) and exhibits extensive blue in inset, which can be explained by the generation of hydroxyl radicals (·OH) originated from H_2O_2 catalyzed by the POD-like catalytic properties of Au@Pd core-shell nanooctahedra nanozyme. On the contrary, there is no peak at 652 nm and no change of color exhibiting in the solution just containing TMB+H_2O_2 (curve a) or TMB+Au@Pd+core-shell nanooctahedra nanozyme (curve b), which is perfectly consistent with the colorimetric photographs presented in the inset in Fig. 2A. As shown in Fig. 2B, the electron paramagnetic resonance (EPR) spec-

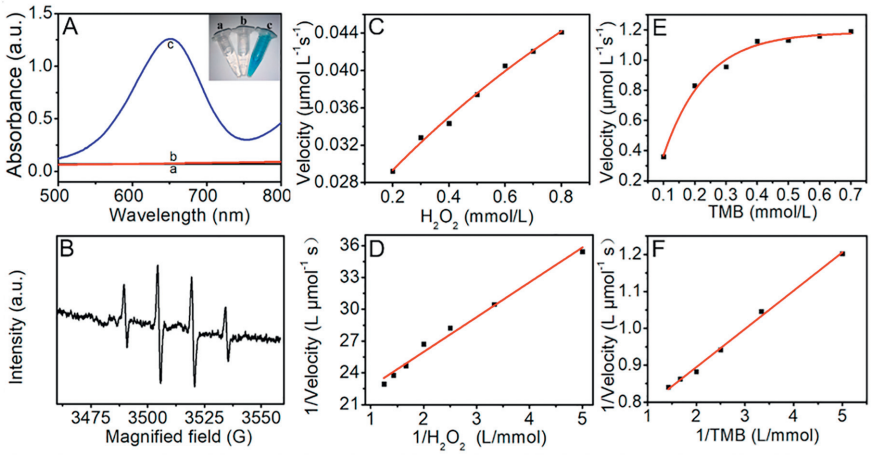

Fig. 2. (A) UV–vis spectra for characterizing POD-like activity: (a) TMB+ H_2O_2 solution, (b) TMB+Au@Pd core-shell nanooctahedra nanozyme solution, (c) TMB+Au@Pd core-shell nanooctahedra nanozyme+H_2O_2 solution. (B) EPR spectra for verifying the generation of ·OH. Steady-state kinetics analysis of Au@Pd nanozyme towards H_2O_2 (C) and TMB (E), and corresponding double-reciprocal Lineweaver-Burk plots of H_2O_2 (D) and TMB (F), respectively.

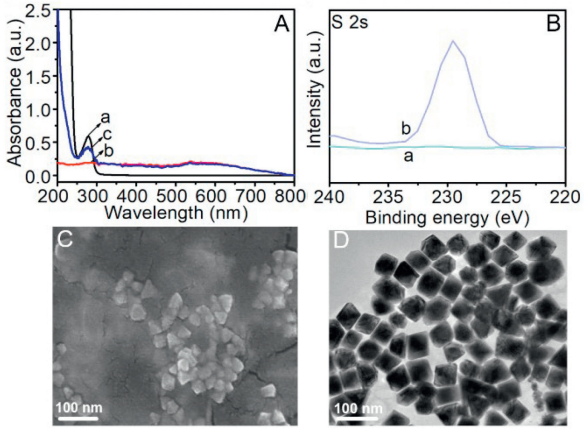

Fig. 3. (A) UV–vis spectroscopy of (a) Ab_2, (b) Au@Pd core-shell nanooctahedra nanozyme, (c) Au@Pd- Ab_2. (B) XPS spectroscopy of Au@Pd (a) and Au@Pd-Ab_2(b). (C) SEM image of Au@Pd-Ab_2. (D) TEM image of Au@Pd-Ab_2.

tra showed the characteristic spectrum of ·OH with a four-line spectrum of 1:2:2:1 intensity, which can confirm the generation of ·OH catalyzed by Au@Pd core-shell nanooctahedra nanozyme with the presence of H_2O_2. According to the Lambert-Beer theory and Michaelis-Menten equation, the steady-state kinetics parameters of Au@Pd nanozyme towards H_2O_2 and TMB was calculated. The steady-state kinetics curves and corresponding double-reciprocal plots for H_2O_2 and TMB were exhibited in Figs. 2C-F, and the K_m and V_{max} of H_2O_2 and TMB for Au@Pd nanozyme were listed in Table S1 (Supporting information). The lower K_m represents the higher enzyme affinity to the substrate, and the higher V_{max} suggests higher catalytical performance. As shown in Table S1 (Supporting information), the prepared Au@Pd nanozyme possesses lower K_m value and higher V_{max} *versus* H_2O_2 and TMB in comparison with HRP and other nanozymes. All the above experimental phenomenon demonstrates that Au@Pd core-shell nanooctahedra nanozyme is of superior POD-like activity. The excellent POD-like activity can be ascribed to the synergistic effect of Au and Pd elements, as well as the special structure of Au@Pd with Au as core and Pd as shell.

The preparation of nanozyme probe plays crucial role in construction of sensitive SPR immunoassay. As illustrated in Figs. 3A-D, the successful formation of Au@Pd-Ab_2 probe was confirmed *via* UV–vis spectra, XPS spectra, SEM and TEM images. It can be seen from Fig. 3A that there is an obvious characterization adsorption peak of protein at 279 nm attributed to secondary antibody (Ab_2) (curve a). In addition, a weak adsorption peak of Au@Pd core-shell nanooctahedra nanozyme presented at 550 nm (curve b) belongs to adsorption of Au. Satisfactorily, two characterization adsorption peaks of protein and Au@Pd core-shell nanooctahedra nanozyme were observed at 279 nm and 550 nm separately, which can be attributed to protein and Au@Pd core-shell nanooctahedra nanozyme depicted in curve c, suggesting that Ab_2 is immobilized on Au@Pd core-shell nanooctahedra nanozyme successfully. In Fig. 3B, compared to Au@Pd nanozyme (curve a), XPS spectra of Au@Pd-Ab_2 (curve b) exhibits a characteristic peak at 229.48 eV corresponding to S 2s, which can be attributed to S species of cysteine residues in proteins. Figs. 3C and D show the SEM and TEM images of Au@Pd core-shell nanooctahedra nanozyme modified antibodies. It can be observed that antibody-loaded Au@Pd core-shell nanooctahedra nanozyme shows different morphology in comparison with unmodified Au@Pd (Figs. 1A and B), and there are some aggregations of Au@Pd core-shell nanooctahedra nanozyme owing to the immobilization of Ab_2. These results indicate the successful preparation of Au@Pd nanozyme probe.

Taking advantage of the good interaction of Staphylococcal protein A (SPA) and Fc fragments of IgG molecules, SPA was utilized to functionalize the sensor chip to effectively immobilize antibodies. As illustrated in Scheme 1B, SPA, Rabbit anti-HigG (Ab_1) and BSA were injected in sequence to fabricate the sensing surface accompanying with washing *via* PBS after each injection. As described in Fig. 4, a system of control experiments for detecting HIgG was designed to elucidate the feasibility of the fabricated SPR immunosensor. In the absence of Au@Pd-Ab_2, Ab_2 was injected to interact with HIgG, which exhibits a weak shift of SPR signal of 0.0313° with the addition of mixture containing aniline and H_2O_2 (Fig. 4A). Replacing 1.0 μg/mL HIgG with 0.01 mol/L PBS, Au@Pd-Ab_2 and mixture were introduced in sequence leading a SPR signal shift of 0.0432°, which can be attributed to the polymerization of aniline catalyzed by the surviving Au@Pd-Ab_2 (Fig. 4B). In the presence of Au@Pd-Ab_2 but without the mixture of aniline and H_2O_2, the resonance angle showed an apparent shift of 0.1017° owing to the combination of HIgG and probe (Fig. 4C). As desired, the resonance angle presented a remarkable shift of 0.4536° compared to Fig. 4C, which is ascribed to the POD-like activity of Au@Pd-Ab_2 for catalyzing the polymerization of aniline with the existence of H_2O_2 to form the second signal amplification based on the immune reaction between HIgG and probe (Fig. 4D). Moreover, SEM images of bare Au chip, formation of polyaniline catalyzed by

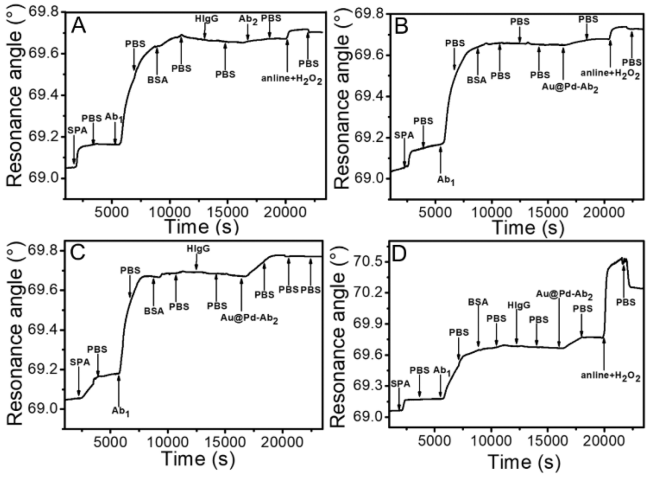

Fig. 4. The feasibility of the constructed SPR immunosensor. (A) Injecting 1.0 μg/mL HIgG and Ab_2 with the mixture of aniline and H_2O_2; (B) adding 0 μg/mL HIgG and Au@Pd-Ab_2 with the mixture of aniline and H_2O_2; (C) in the presence of 1.0 μg/mL HIgG and Au@Pd-Ab_2 with the absence of aniline and H_2O_2; (D) in the presence of 1.0 μg/mL HIgG, Au@Pd-Ab_2, aniline and H_2O_2.

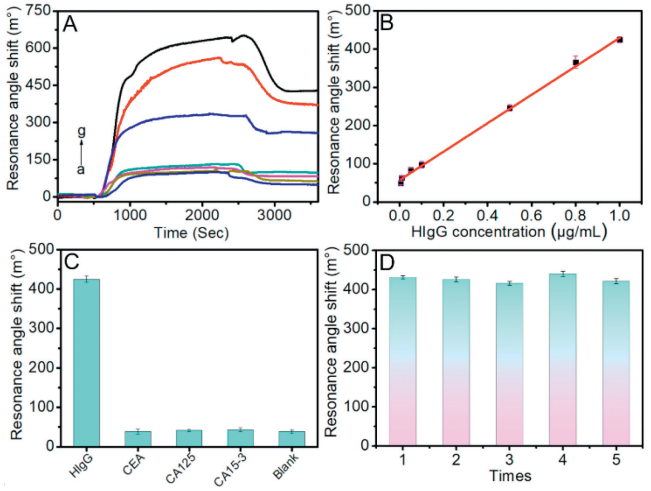

Fig. 5. (A) The sensorgram of different concentration (from a-g) of HIgG detected *via* SPR immunosensor. (B) The calibration curve of the proposed strategy for HIgG determination. (C) SPR response of 1.0 μg/mL HIgG, 25 U/mL CEA, 25 U/mL CA125, 30 U/mL CA15-3 and blank solution for studying the selectivity of the fabricated SPR immunosensor. (D) SPR response of the proposed immunosensor after being used several times for investigating the repeatability of the immunosensor.

Au@Pd core-shell nanooctahedra nanozyme with the presence of H_2O_2 on the Au chip surface were studied in Fig. S2 (Supporting information) showed smooth Au surface, while Fig. S2B (Supporting information) presented different morphology with long band shape with sharp needle-like polymers appearing on the Au chip surface, which demonstrates the formation of polyaniline. In addition, NMR-spectra were also conducted to verify the formation of polyaniline catalyzed by Au@Pd nanozyme (Fig. S3 in Supporting information). The polymerization reaction triggered by Au@Pd nanozyme probe can be illustrated as follows. The O–O bond of H_2O_2 breaks to form ·OH in the catalysis process of H_2O_2 catalyzed by Au@Pd nanozyme with POD-like activity. Then, the generated ·OH oxidized the amino groups in aniline to form radicals that can interact with other aniline molecules to activate polymerization of aniline to generate polyaniline. In general, benefiting from the above experimental results, the proposed nanozyme-induced signal amplification strategy in SPR immunosensor was proven to work.

The proposed nanozyme-triggered polymerization amplification strategy for signal amplification was utilized to design SPR immunosensor to determine HIgG under optimal condition (Fig. S4 in Supporting information). It can be observed from Fig. 5A, the resonance angle shifts apparently with the elevation of the concentration of HIgG, which is attributed to the signal enhancement from the polymerization of aniline catalyzed by POD-like activity of Au@Pd-Ab_2 probe. An evident linear relationship of resonance angle shifts *versus* the concentration of HIgG was presented in Fig. 5B and the constructed immunosensor possesses a wide linear range of 0.005–1.0 μg/mL with low detection limit of 0.106 ng/mL, which is much lower than that of other reported SPR sensors (Table S2 in Supporting information).

As shown in Fig. 5C, the resonance angle shifts were recorded with the respective injection of HIgG (1.0 μg/mL), CEA (25 U/mL), CA15–3 (30 U/mL), CA125 (25 U/mL) and PBS, which explored the anti-interference property of the fabricated immunosensor. It is obvious that the addition of HIgG leads to a more conspicuous resonance angle shift than that of other antigens, which is consistent with the anticipation. The resultant results suggest that fabricated immunosensor has high specificity for determination of target analytes. The reproducibility was evaluated by recording the resonance angle shift of the same sensor chip that was rinsed with NaOH for regeneration several times. It can be seen from Fig. 5D that SPR signals have no significant change. The SPR signals are 431.5 m°, 426.1 m°, 415.9 m°, 440.2 m°, 421.5 m° within the five-time detection and the relative standard deviation was calculated to be 2.0%, which demonstrates that the proposed immunosensor shows excellent repeatability.

For assessing the applicability of the designed strategy for HIgG in clinical samples, recovery experiments were performed by spiking HIgG at various concentrations into serum samples without any treatments. Ethical approval was obtained from the Ethics Committee of Northern Jiangsu People's Hospital. In addition, written informed consent was obtained from all the participants prior for this study. HIgG with different concentrations of 0.10 μg/mL, 0.50 μg/mL, 1.00 μg/mL was mixed with three serum samples separately. As described in Table S3 (Supporting information), there was good consistence between the added and detected values of HIgG contents, and the range of recovery rates were calculated about 96.3%–106.4%, demonstrating no significant interference in clinical samples. In general, the proposed SPR immunosensor with good reproducibility and reliability based on Au@Pd-Ab_2 probe can be exploited to determine HIgG in human serum quantitatively. To sum up, the constructed SPR immunosensor has the advantages of high sensitivity, low detection limit, and low sample consumption, as well as good specificity and reproducibility, and good practicality.

In conclusion, a highly sensitive SPR immunosensor was fabricated based on a nanozyme-triggered polymerization amplification strategy. Au@Pd core-shell nanooctahedra nanozyme was simply synthesized and shows excellent POD-like activity, which was further exploited to immobilize secondary antibodies as SPR label probe. More attractively, Au@Pd nanozyme with intrinsic POD-like activity can catalyze H_2O_2 to ·OH, which triggered the polymerization of aniline to form polyaniline, greatly enhancing the sensitivity of SPR immunosensor. Moreover, taking HIgG as model, the nanozyme signal-amplified SPR immunosensor shows excellent analytical properties for determining HIgG. The proposed strategy compensates the shortcoming of current signal amplification methods such as the use of natural enzymes and relatively complex amplifying process. This research provides new sights on establishing sensitive SPR immunosensor for biomarkers and may evokes more inspiration for developing signal amplification methods based on nanozymes in biosensing fields.

Declaration of competing interest

The authors declare that they have no known competing financial interests or personal relationships that could have appeared to influence the work reported in this article.

CRediT authorship contribution statement

Feng Shi: Writing – original draft, Software, Methodology, Investigation, Formal analysis. **Guiling Li:** Supervision, Software, Investigation. **Haibing Zhu:** Software, Investigation, Formal analysis. **Ming Chen:** Supervision, Conceptualization. **Juan Li:** Supervision, Methodology. **Huifang Shen:** Methodology, Formal analysis. **Hao Zeng:** Supervision, Software. **Lingfeng Min:** Validation, Supervision, Methodology, Conceptualization. **Zhanjun Yang:** Writing – review & editing, Supervision, Methodology, Conceptualization.

Acknowledgments

This work was financially supported by National Natural Science Foundation of China (Nos. 22474124, 21575125), the National Natural Science Foundation of Jiangsu Province (No. BK20221370), Key University Natural Science Foundation of Jiangsu-Province (No. 20KJA150004), the Project for Science and Technology of Yangzhou (No. YZ2022074), Project for Yangzhou City and Yangzhou University corporation (No. YZ2023204), the Open Research Fund of State Key Laboratory of Analytical Chemistry for Life Science (No.SKLACLS2405), and Postgraduate Research & Practice Innovation Program of Jiangsu Province (No. KYCX22_3462).

Supplementary materials

Supplementary material associated with this article can be found, in the online version, at doi:10.1016/j.cclet.2024.110333.

References

[1] Y.Y. Huang, J.S. Ren, X.G. Qu, Chem. Rev. 119 (2019) 4357–4412.
[2] L.M. Zheng, F.Q. Wang, C.R. Jiang, et al., Coordin. Chem. Rev. 471 (2022) 214760.
[3] Y.J. Dai, Y.M. Ding, L.L. Li, Chin. Chem. Lett. 32 (2021) 2715–2728.
[4] W.P. Yang, X. Yang, L.J. Zhu, et al., Coordin. Chem. Rev. 448 (2021) 214170.
[5] J.J. Luo, R.L. Liu, S.C. Zhao, Y. Gao, J. Anal. Test. 7 (2023) 53–68.
[6] L. Han, H.J. Zhang, D.Y. Chen, F. Li, Adv. Funct. Mater. 28 (2018) 1800018.
[7] J.H. Ju, Y.T. Chen, Z.Q. Liu, et al., Chin. Chem. Lett. 34 (2023) 107820.
[8] H.Y. Li, S.X. Zhao, Z.X. Wang, F. Li, Small 19 (2023) 2206465.
[9] L.W. Wang, F.N. Gao, A.Z. Wang, et al., Adv. Mater. 32 (2020) 2005423.
[10] Y.H. Zhong, X. Tang, J. Li, et al., Chem. Comun. 54 (2018) 13813.
[11] X. Huang, S.T. Zhang, Y.J. Tang, et al., Coordin. Chem. Rev. 449 (2021) 214216.
[12] Y.H. Xia, K.M. Sun, Y.N. Zuo, S.Y. Zhu, X.E. Zhao, Chin. Chem. Lett. 33 (2022) 2081–2085.
[13] T. Hou, N.N. Xu, X. Song, et al., Chin. Chem. Lett. 34 (2023) 107907.
[14] J.X. Xiao, F. Shi, Y. Zhang, et al., Chem. Commun. 60 (2024) 996–999.
[15] D.Q. Zhu, M.L. Zhang, L. Pu, P.P. Gai, F. Li, Small 18 (2022) 2104993.
[16] W.H. Gao, J.Y. He, L. Chen, et al., Nat. Commun. 2023 (14) (2023) 160.
[17] L. Yao, M.M. Zhao, Q.W. Luo, et al., ACS Nano 16 (2022) 9228–9239.
[18] J.Q. Chen, X.Y. Liu, G.C. Zheng, et al., Small 19 (2023) 2205924.
[19] J.X. Chen, Q. Ma, M.H. Li, et al., Nat. Commun. 12 (2021) 3375.
[20] Y.J. Tang, Y. Wu, W.Q. Xu, et al., Anal. Chem. 94 (2022) 1022–1028.
[21] W. Cao, J.S. Lin, F. Muhammad, et al., J. Anal. Test. 3 (2019) 253–259.
[22] J.H. Zhou, H.W. Gou, T.J. Zhao, et al., Biosens. Bioelectron. 203 (2022) 114048.
[23] Y.P. Xia, F. Shi, R.X. Liu, et al., Anal. Chem. 96 (2024) 1345–1353.
[24] O. Adeniyi, S. Sicwetsha, P. Mashazi, ACS Appl. Mater. Interfaces 12 (2020) 1973–1987.
[25] J.Y. Zhan, F. Shi, J. Li, et al., Chin. Chem. Lett. 34 (2023) 108791.
[26] F. Shi, M.Y. Peng, H.B. Zhu, et al., Anal. Chem. 95 (2023) 14516–14520.
[27] Z.Z. Xu, B.F. Xu, A.P. Tanjung, et al., Sens. Actuators B: Chem. 412 (2024) 135732.
[28] Q.Y. Ai, B.F. Xu, F. Xu, et al., Talanta 274 (2024) 126034.
[29] Q. Wang, Z.H. Ren, W.M. Zhao, et al., Nanoscale 14 (2022) 564–591.
[30] L.K. Chin, T. Son, J.S. Hong, et al., ACS Nano 14 (2020) 14528–14548.
[31] B.Y. Zhu, J. Yang, R. Van, et al., Chem. Sci. 13 (2022) 8104–8116.
[32] C.E. Froehlich, J.Y. He, C.L. Haynes, Anal. Chem. 95 (2023) 2639–2644.
[33] A. Shamsi, D. DasGupta, F.A. Alhumaydhi, et al., RSC Med. Chem. 13 (2022) 737–745.
[34] A. Azzouz, L. Hejjii, K.H. Kim, et al., Biosens. Bioelectron. 197 (2022) 113767.
[35] T.Y. Xue, W.Y. Liang, Y.W. Li, et al., Nat. Commun. 10 (2019) 28.
[36] A. Philip, A.R. Kumar, Coord. Chem. Rev. 458 (2020) 214424.
[37] T.T. Goodrich, H.J. Lee, R.M. Corn, J. Am. Chem. Soc. 126 (2004) 4086–4087.
[38] Y. Li, J. Lee, R.M. Corn, Anal. Chem. 79 (2007) 1082–1088.
[39] Y. Liu, Y. Dong, J. Jauw, M.J. Linman, Q. Cheng, Anal. Chem. 82 (2010) 3679–3685.
[40] Y. Liu, Q. Cheng, Anal. Chem. 84 (2012) 3179–3186.
[41] C.Y. Song, X.Y. Jiang, Y.J. Yang, et al., ACS Appl. Mater. Interfaces 12 (2020) 31242–31254.
[42] X. Su, H.F. Teh, K.M. Aung, Y. Zong, Z. Gao, Biosens. Bioelectron. 23 (2008) 1715–1720.
[43] P.X. Yuan, S.Y. Deng, C.G. Yao, Y. Wan, S. Cosnier, Biosens. Bioelectron. 89 (2017) 319–325.
[44] C. Li, H.L. Zhu, Y. Guo, et al., ACS Sens. 7 (2022) 2778–2787.